studies of **5** in $CD_2Cl_2$ solution. The $^1H$ NMR spectra of **5** with acetone-$d_6$ as solvent were invariant over the temperature range of −85 to +25 °C and were similar to that obtained in $CD_2Cl_2$, with only minor shifts in peak positions.

The $^1H$ NMR spectrum of **5** with $CD_3CN$ as solvent at 25 °C was complex and provided evidence for a $C_1$ isomer of **5** with no detectable resonances due to the $C_3$isomer. The presence of a triplet at $\delta$ −5.85 ($J_{P-H}$ = 72 Hz) and absence of the quartet at $\delta$ −1.96 due to H1 are consistent with the presence of a doubly bridging hydride that is trans to two phosphorus atoms and support the presence of an acetonitrile adduct of **5**. There were also large resonances between −20 and −26 ppm that may be due to the six nonequivalent terminal hydrides expected in a $C_1$ isomer; however, the spectrum was very complex possibly due to the presence of other hydride species. Therefore, the resonances were not assigned.

Since complex **5** is believed to contain two sets of terminal hydrides, the Ir atoms are coordinatively unsaturated relative to the Ir atoms in complex **1**. In light of the reactivity of **1** with coordinating solvents and two-electron donors, it is not surprising that **5** reacts with acetontrile. It was similarly expected that **5** would form an adduct with acetone; however, no conclusive evidence for such an adduct was obtained.

The deuterium analogue of **5** was synthesized in a manner analogous to that for **5**, with $D_2$ and $CH_3OD$ as solvent. Attempts to synthesize this with $D_2$ and $CH_3OH$ as solvent were unsuccessful and resulted only in the formation of **5**. Furthermore, refluxing **5** in $CH_3OD$ did not result in H/D exchange as determined by IR spectroscopy. Similar results were observed for **1** and its deuterium analogue.[20,35] These results imply that one of the precursors to **5** undergoes H/D exchange with $CH_3OD$. For complex **1**, it was proposed that the intermediate *cis*-[Ir(dppp)$(H)_2$(solvent)$_2]^+$ underwent H/D exchange with protic solvents such as $CH_3OD$. This intermediate was detected in $^1H$ NMR studies of the hydrogenation of [Ir(dppp)(COD)]$^+$ in acetone solution.[45] It is likely that a similar hydride species, *cis*-[Ir(PN)$(H)_2$(solvent)$_2]^+$, also undergoes H/D exchange with $CH_3OD$; however, no attempts to identify such an intermediate have been carried out for this system.

**Acknowledgment.** This work was supported by the National Science Foundation. We gratefully acknowledge the Johnson Matthey Co. for a generous loan of $IrCl_3$. A.L.C. also thanks the National Science Foundation for a Graduate Fellowship.

**Registry No.** **1**, 73178-86-6; **2**$(BF_4)_2$, 112021-56-4; **2**$(BF_4)_2\cdot 2C_2H_4Cl_2$, 112067-95-5; **3**$(BF_4)_2$, 112021-52-0; **4**$(PF_6)$, 112021-45-1; **5**$(PF_6)_2$, 112021-47-3; **5**$(PF_6)_2\cdot C_6H_6O$, 112068-61-8; **5**$(BF_4)_2$, 112021-48-4; [$Ir_3$(dppp)$_3(D)_7(CO)$][$BF_4)_2$, 112021-58-6; [$Ir_3$(dppp)$_3(D)_7$-$(CH_3C_6H_4NC)$][$BF_4)_2$, 112021-54-2; [Ir(COD)Cl]$_2$, 12112-67-3; [$Ir_3$-$(PN)_3(D)_7$][$PF_6)_2$, 112021-50-8.

**Supplementary Material Available:** ORTEP drawings of **2** and **5** and listings of distances and angles, general temperature factor expressions, final positional and thermal parameters for all atoms including counterions and solvate molecules, calculated hydrogen atom positions, and least-squares planes (28 pages); listings of observed and calculated structure factor amplitudes (70 pages). Ordering information is given on any current masthead page.

(45) $H_2$ was bubbled through an acetone solution of [Ir(dppp)(COD)]$^+$ in an NMR tube at −78 °C, resulting in a color change from burgundy to yellow indicative of the intermediate *cis*-[Ir$(H)_2$(dppp)(COD)]$^+$. $^1H$ NMR (acetone-$d_6$, −70 °C, 270 MHz): $\delta$ −9.80 (d of d, $J$ = 85 and 10 Hz), −12.5 (t, $J$ = 14 Hz). $^{31}P$ NMR: ($CH_2Cl_2$, −74 °C, 40.5 MHz): $\delta$ −14.07 (d, $J$ = 31 Hz), −29.05 (d of d, $J$ = 31 and 20 Hz). This solution was then warmed to 25 °C for ca. 3 min and shown to contain, as one of the major products, *cis*-[Ir$(H)_2$(dppp)(solvent)$_2]^+$. $^1H$ NMR (acetone-$d_6$, 25 °C, 270 MHz): $\delta$ −25.14 (t, $J$ = 21 Hz). Other resonances observed in this reaction mixture were not identified but probably resulted from species in which COD was partially hydrogenated.

Contribution from the Department of Chemistry, Wayne State University, Detroit, Michigan 48202

# Synthesis and Spectroscopic and Redox Properties of Binuclear Copper(II) Ketimine Schiff-Base Complexes. Further Studies of a Novel Class of $\pi$-Molecular Complexes Derived from Binuclear Copper(II) Complexes

R. L. Lintvedt,* K. A. Rupp, and Mary Jane Heeg

*Received November 26, 1986*

The preparation, spectral properties, and redox characteristics of a series of copper(II) Schiff-base complexes are reported. The series consists of dinuclear copper(II) complexes of the 2,2-dimethyl-7-((4-X-phenyl)imino)-3,5-octanedionato ligand where X = $OCH_3$, $CH_3$, H, Cl, Br, or $NO_2$ and the ligand 2,2-dimethyl-7-(X-imino)-3,5-octanedionato where X = methyl, ethyl, *n*-propyl, or *n*-butyl. A Hammett plot, for the former, of $E_{1/2}$ vs $2\sigma_p$ is linear and has a slope of 0.08. The complexes are rigorously diamagnetic at room temperature, which allows $^1H$ NMR data to be obtained. Unusual chemical shifts are observed due to anisotropy generated by the aromatic ketimine substituent and the presence of the copper(II) center. The structures of bis[2,2-dimethyl-7-(ethylimino)-3,5-octanedionato]dicopper(II)$-{}^1/_2$-benzene, $Cu_2$(PAAet)$_2\cdot{}^1/_2C_6H_6$, and bis[2,2-dimethyl-7-(*n*-propylimino)-3,5-octanedionato]dicopper(II), $Cu_2$(PAApr)$_2$, have been determined by X-ray diffraction. The former is composed of stacks of benzene molecules sandwiched between the copper complexes in an ADAADA... pattern. Crystal data are as follows: $P\bar{1}$; $a$ = 9.438 (4), $b$ = 13.323 (2), $c$ = 11.384 (1) Å; $\alpha$ = 75.68 (1), $\beta$ = 89.68 (2), $\gamma$ = 82.34 (2)°; $Z$ = 2; $R$ = 0.039 and $R_w$ = 0.054 for 3824 observed reflections. $Cu_2$(PAApr)$_2$ consists of the nonsolvated molecule centered on an inversion center in the space group $P2_1/c$. Crystal data are as follows: $a$ = 11.277 (6), $b$ = 6.249 (1), $c$ = 19.237 (3) Å; $\beta$ = 94.47 (3)°; $Z$ = 2; $R$ = 0.030 and $R_w$ = 0.038 for 1771 observed reflections. The structural parameters for these compounds are compared with those of the more highly solvated molecules $Cu_2$(PAAan)$_2\cdot C_6H_6$ and $Cu_2$(PAApnan)$_2\cdot 2C_6H_6$ and are discussed in light of a $\pi$-molecular interaction between solvent and complex.

## Introduction

An important development in the field of coordination chemistry has been the design and synthesis of ligands capable of binding two or more transition-metal ions. Examples of such ligand systems include monocyclic[1] and bicyclic[2] hexaamines, cyclic[3] and acyclic[4] Schiff bases, polycyclic "cryptands",[5] "earmuffs",[6] and "wishbones",[7] "face-to-face",[8] "capped",[9] and "crowned"[10] por-

(1) Coughlin, P. K.; Lippard, S. J. *J. Am. Chem. Soc.* **1981**, *103*, 3228. Martin, A. E.; Bulkowski, J. E. *J. Org. Chem.* **1982**, *47*, 415.
(2) Martin, A. E.; Bulkowski, J. E. *J. Am. Chem. Soc.* **1982**, *104*, 1434.
(3) Gagne, R. R.; Koval, C. A.; Smith, T. J.; Cimolino, M. C. *J. Am. Chem. Soc.* **1979**, *101*, 4571. Nelson, S. M. *Pure Appl. Chem.* **1980**, *52*, 2461.
(4) Robson, R. *Aust. J. Chem.* **1970**, *23*, 2217. Grzybowski, J. J.; Merrell, P. H.; Urbach, F. L. *Inorg. Chem.* **1978**, *17*, 3078.
(5) Gisselbrecht, J. P.; Gross, M.; Alberts, A. H.; Lehn, J. M. *Inorg. Chem.* **1980**, *19*, 1386. Louis, R.; Agnus, Y.; Weiss, R. *J. Am. Chem. Soc.* **1978**, *100*, 3604.

0020-1669/88/1327-0331$01.50/0 © 1988 American Chemical Society

phyrins, and the β-polyketones.[11] Much of the interest in multimetal complexes originates from their potential as models for metalloproteins. In particular, the binuclear metal complexes are of interest because it is known, or believed, that many of the biological functions performed by certain metalloproteins are consequences of the metal centers occurring in pairs.[12]

For some time, our efforts have been aimed at the bis(1,3,5-triketonato)dimetal complexes and their diimine Schiff-base derivatives.[13] The binuclear Cu(II) complexes prepared from 1,3,5-triketones in which one terminal carbonyl oxygen is replaced by a nitrogen is an example of a second type of Schiff-base derivative.[14] The ease in modification of the alkyl or aromatic substituent attached to the nitrogen provides a systematic way of probing the structural, electrochemical, and spectroscopic properties of the complexes.

In a previous paper[14] we reported a new type of π-molecular complex containing a binuclear copper(II) complex and benzene. The two complexes examined are examples of the two most common types encountered, ADAD... and DADDAD..., where the distance between the parallel benzene and complex is 3.26 Å. With the structures determined herein, we have completed a series of π-molecular complexes consisting of a benzene donor and a dicopper(II) Schiff-base acceptor with the unique stacking pattern of ADAADA....

## Experimental Section

**I. Synthesis.** Solid primary amines were recrystallized from water/methanol mixtures, while liquid primary amines were distilled under vacuum before use. Solvents used were of reagent grade.

**A. Triketone.** $H_2PAA$, 2,2-dimethyl-3,5,7-octanetrione, was prepared by a method previously described.[15]

**B. $H_2PAA$ Ketimines and Their Copper Complexes. Method A.** To 100 mL of refluxing absolute methanol were added one drop of concentrated $H_2SO_4$ and 2.0 g (10.9 mmol) of $H_2PAA$. Upon addition of a 10% molar excess (12.0 mmol) of primary amine, the yellow color of the solution intensified. The solution was refluxed 20 min, and the solvent was removed under reduced pressure. The residues were orange-yellow oils.

The crude ligand was redissolved in 20 mL of methanol and added dropwise to 100 mL of a refluxing solution of methanol containing 2.18 g (10.9 mmol) of copper acetate monohydrate. If a dark green precipitate did not form immediately, 2.0 mL (14.3 mmol) of triethylamine was added to enhance complexation. The solution was reduced in volume and filtered while warm, and the green solids were washed with methanol and air-dried.

**Method B.** A solution was prepared by adding 1.5 mL (8.3 mmol) of $H_2PAA$ and one drop of concentrated $H_2SO_4$ to 100 mL of refluxing methanol. The appropriate primary amine (9.6 mmol) was added, intensifying the solution color. The solution was allowed to reflux 20 min. Slow evaporation of the solvent yielded an oil. The ligand was used in this form without further purification.

The ligand described above was dissolved in 10 mL of methanol and added dropwise to a refluxing solution of 1.66 g (8.3 mmol) of copper acetate in 100 mL of methanol. Upon addition of 2.0 mL (14.3 mmol) of triethylamine, a very fine, dark green precipitate formed. The solution was refluxed 0.5 h and filtered while warm, and the dark green microcrystalline product was washed with methanol and air-dried.

**Method C.** A solution of 2.01 g (10.9 mmol) of $H_2PAA$, three drops of concentrated $H_2SO_4$, and 1.51 g (10.9 mmol) of *p*-nitroaniline in 120 mL of toluene was refluxed 2.5 h in a 250-mL flask fitted with a Dean–Stark trap. The toluene was removed under reduced pressure. An orange-yellow crystalline product was obtained and used without further purification.

The crude ligand was redissolved in 25 mL of chloroform, and the solution was added dropwise to a refluxing methanol solution containing 2.18 g (10.9 mmol) of copper acetate. A very fine, green precipitate formed immediately. The solution was refluxed 20 min and filtered while warm. A dark olive green microcrystalline product was recovered.

All of the above complexes were soluble in organic solvent such as chloroform, *N*,*N*-dimethylformamide, hexanes, benzene, and benzene derivatives. Suitable crystals for X-ray analysis were obtained by crystallization from benzene and hexanes.

**Table I.** Elemental Analyses and Synthetic Methods for the Bis[2,2-dimethyl-7-(R-imino)-3,5-octanedionato]dicopper(II) Complexes

| R | | % C | % H | % N | % Cu | % X | method |
|---|---|---|---|---|---|---|---|
| $CH_3$ | calcd | 51.05 | 6.62 | 4.41 | 24.55 | | B |
| | obsd | 51.39 | 6.40 | 4.64 | 24.57 | | |
| $CH_3CH_2$ | calcd | 52.83 | 7.02 | 5.13 | 23.29 | | B |
| | obsd | 52.53 | 6.98 | 5.03 | 23.06 | | |
| $n$-$C_3H_7$ | calcd | 54.43 | 7.38 | 4.88 | 22.15 | | A |
| | obsd | 54.08 | 7.54 | 4.28 | 21.76 | | |
| $n$-$C_4H_9$ | calcd | 55.89 | 7.70 | 4.66 | 21.12 | | A |
| | obsd | 56.37 | 7.75 | 4.75 | 20.33 | | |
| $C_6H_5$ | calcd | 59.89 | 5.97 | 4.37 | 19.80 | | B, C |
| | obsd | 59.65 | 6.05 | 4.12 | 19.51 | | |
| | calcd | 60.97 | 6.32 | 4.18 | 18.97 | | A |
| | obsd | 60.87 | 6.41 | 4.14 | 19.24 | | |
| $p$-$C_6H_4OCH_3$ | calcd | 58.19 | 6.03 | 3.99 | 18.11 | | B |
| | obsd | 58.28 | 6.31 | 4.09 | 17.94 | | |
| $p$-$C_6H_4NO_2$ | calcd | 52.52 | 4.96 | 7.66 | 17.37 | | C |
| | obsd | 52.58 | 5.06 | 7.50 | 17.01 | | |
| $p$-$C_6H_4Cl$ | calcd | 54.08 | 5.11 | 3.94 | 17.88 | 9.98 | A |
| | obsd | 53.82 | 5.20 | 3.84 | 17.55 | 10.06 | |
| $p$-$C_6H_4Br$ | calcd | 48.07 | 4.54 | 3.50 | 15.90 | 19.99 | A |
| | obsd | 47.40 | 4.48 | 3.61 | 15.47 | 20.04 | |
| $p$-$C_6H_4CF$ | calcd | 52.51 | 4.67 | 3.60 | 16.34 | 14.66 | A |
| | obsd | 52.36 | 4.76 | 3.41 | 16.00 | 14.76 | |

**II. Physical and Chemical Measurements.** Chemical analyses were performed by Galbraith Laboratories, Inc., Knoxville, TN. The results of elemental analysis are presented in Table I. Infrared spectra were recorded on a Nicolet 20DX Fourier transform spectrometer using KBr pellets. Melting points were recorded uncorrected on a Thomas Hoover melting point apparatus. Electronic absorption spectra in the visible and ultraviolet regions were recorded on a Perkin-Elmer Lambda 3B spectrometer with a 3600 data station. The spectra were obtained in spectrophotometric grade toluene, chloroform, and *N*,*N*-dimethylformamide with concentration ranges of 0.61–3.07 mmol.

Nuclear magnetic resonance spectra were recorded in the pulsed Fourier transform mode on a General Electric QE-300 spectrometer. Chemical shifts were recorded relative to that of chloroform (7.26 ppm). Magnetic susceptibilities were measured at room temperature by the Faraday method using $Hg[Co(SCN)_4]$ as a calibrant.[16] Pascal's constants were used for diamagnetic corrections.[17]

Electrochemical results were obtained with a Princeton Applied Research Model 173 potentiostat/galvanostat equipped with a PAR Model 179 digital coulometer and Model 175 universal programmer. Data collection and output were accomplished with a Nicolet digital oscilloscope, Model 2090-3C, in conjunction with a Data General Eclipse S-130 minicomputer. Computer programs for data transfer were designed in this laboratory. Electrochemical measurements were made in high-purity grade (Burdick and Jackson) *N*,*N*-dimethylformamide (DMF), which

(6) Burk, P. L.; Osborn, J. A.; Youinou, M. T.; Angus, Y.; Louis, R.; Weiss, R. *J. Am. Chem. Soc.* **1981**, *103*, 1273.
(7) Karlin, K. D.; Dahlstrom, P. L.; DiPierro, L. T.; Simon, R. A.; Zubieta, J. *J. Coord. Chem.* **1981**, *11*, 61. Taqui Kahn, M. M.; Mohiuddin, R.; Ahmed, M.; Martell, A. E. *J. Coord. Chem.* **1980**, *10*, 1.
(8) Collman, J. P.; Marrocco, M.; Denisevich, P.; Koval, C.; Anson, F. C. *J. Electroanal. Chem. Interfacial Electrochem.* **1979**, *101*, 117. Collman, J. P.; Denisovich, P.; Konai, Y.; Marrocco, M.; Koval, C.; Anson, F. C. *J. Am. Chem. Soc.* **1980**, *102*, 117.
(9) Buckingham, D. A.; Gunter, J. J.; Mander, L. N. *J. Am. Chem. Soc.* **1978**, *100*, 2899.
(10) Chang, C. K. *J. Am. Chem. Soc.* **1977**, *99*, 2819.
(11) Lintvedt, R. L.; Guthrie, J. W.; Glick, M. D. *Inorg. Chem.* **1980**, *19*, 2949. Lintvedt, R. L.; Ceccarelli, C.; Glick, M. D.; Schoenfelner, B. A. *Inorg. Chem.* **1984**, *23*, 2867.
(12) Lontie, R. In *Inorganic Biochemistry*; Eichhorn, G. L., Ed.; Elsevier: New York, 1973. *The Biochemistry of Copper*; Piesach, J., Aisen, P., Blumberg, W., Eds.; Academic: New York, 1966. Fee, J. A. *Struct. Bonding (Berlin)* **1975**, *23*, 1. Bienart, H. *Coord. Chem. Rev.* **1980**, *33*, 55. Urbach, F. L. *Met. Ions. Biol. Syst.* **1981**, *13*, 73. Solomon, E. I.; Penfield, K. W.; Wilcox, D. E. *Struct. Bonding (Berlin)* **1983**, *53*, 1.
(13) Ahmad, N.; Lintvedt, R. L. *Inorg. Chem.* **1982**, *21*, 2356. Lintvedt, R. L.; Glick, M. D.; Tomlonovic, B. K.; Gavel, D. P. *Inorg. Chem.* **1976**, *15*, 1646. Lintvedt, R. L.; Glick, M. D.; Anderson, T. J.; Mack, J. L. *Inorg. Chem.* **1976**, *15*, 2258.
(14) Wishart, J. F.; Ceccarelli, C.; Lintvedt, R. L.; Berg, J. M.; Foley, D. P.; Frey, T.; Hahn, J. E.; Hodgson, K. O.; Weis, R. *Inorg. Chem.* **1983**, *22*, 1667.
(15) Miles, M. L.; Harris, T. M.; Hauser, C. R. *J. Org. Chem.* **1965**, *30*, 1007.
(16) St. Rade, H. *J. Phys. Chem.* **1973**, *77*, 424.
(17) Bourdreaus, E. A.; Mulay, L. N. *Theory and Applications of Molecular Paramagnetism*; Wiley: New York, 1976.

**Table II.** Experimental Crystallographic Data

| | $Cu_2(PAAet)_2 \cdot {}^1/_2C_6H_6$ | $Cu_2(PAApr)_2$ |
|---|---|---|
| formula | $Cu_2O_4N_2C_{27}H_{41}$ | $Cu_2O_4N_2C_{26}H_{42}$ |
| mol wt | 584.72 | 573.72 |
| cryst dimens, mm | 0.40 × 0.30 × 0.35 | 0.08 × 0.23 × 0.56 |
| cryst system | triclinic | monoclinic |
| space group | $P\bar{1}$ | $P2_1/c$ |
| cell dimens | | |
| $a$, Å | 9.438 (4)[b] | 11.277 (6)[c] |
| $b$, Å | 13.323 (2) | 6.249 (1) |
| $c$, Å | 11.384 (1) | 19.237 (3) |
| $\alpha$, deg | 75.68 (1) | |
| $\beta$, deg | 89.68 (2) | 94.47 (3) |
| $\gamma$, deg | 82.34 (2) | |
| $V$, Å$^3$ | 1373.9 (6) | 1351.4 (7) |
| $Z$ | 2 | 2 |
| $d_{calcd}$, g cm$^{-3}$ | 1.413 | 1.411 |
| scan method | $\theta/2\theta$ | $\theta/2\theta$ |
| scan range, deg: below $K\alpha_1$, above $K\alpha_2$ | 1.0, 1.0 | 1.1, 1.3 |
| scan rate, deg min$^{-1}$ | 2–5 | 2–5 |
| bkgd/scan time | 0.5 | 0.5 |
| $2\theta$ range, deg | 2.5–50 | 3–50 |
| no. of total data | 5389 | 2945 |
| no. of unique data | 4884 | 2403 |
| no. of obsd. data, $I_o \geq 3\sigma(I)$ | 3824 | 1771 |
| $\mu$, cm$^{-1}$ | 16.42 | 16.70 |
| transmission coeff: min, max | 1.515, 1.811 | 0.507, 0.885 |
| $F(000)$ | 614 | 604 |
| $R$, $R_w$[a] for obsd reflcns | 0.039, 0.054 | 0.030, 0.038 |
| $R$, $R_w$ for all reflcns | 0.055, 0.060 | 0.056, 0.049 |
| weight | $(\sigma_F)^{-2}$ | $(\sigma_F)^{-2}$ |

[a] $R_w = [\sum w(|F_o| - |F_c|)^2/\sum wF_o^2]^{1/2}$. [b] Cell constants calculated from 28 high-$2\theta$ reflections measured at both $\pm 2\theta$. [c] Cell constants calculated from 25 high-$2\theta$ reflections constrained to be monoclinic.

was used without further purification. Tetraethylammonium perchlorate (TEAP) was used as a supporting electrolyte (G. F. Smith). Solutions were deoxygenated with ultrahigh-purity $N_2$ that had been passed through a chromous–perchloric acid scrubber, a $CaSO_4$ drying column, and a DMF solution. Cyclic voltammograms were obtained with use of a three-electrode glass cell with a saturated NaCl calomel reference electrode, a Pt-wire counter electrode, and a Brinkmann Model EA 290 hanging-mercury-drop electrode (HMDE). The reference cell was separated from the sample chamber by two salt bridges. The bridge adjacent to the reference electrode contained 0.13 M TEAP aqueous solution, and the one adjacent to the sample chamber contained a 0.1 M TEAP in DMF solution. Tris(1,1,1-trifluoro-2,4-pentanedionato)ruthenium(III) was used as an internal standard and found to have $E_{1/2} = -0.138 \pm 0.005$ V and $\Delta E_p = 60.0 \pm 5.0$ mV under our conditions.[18]

**III. Crystallographic and Structure Determination. $Cu_2(PAAet)_2 \cdot {}^1/_2C_6H_6$.** Brick-shaped crystals of this material were deeply colored, nearly black. A sample mounted on a Nicolet $P2_1$ automated diffractometer indicated the triclinic crystal system. Absorption corrections[19] were applied by the method of indexing crystal faces. Data collection proceeded at room temperature with Mo $K\alpha$ radiation from a graphite monochromator. The structure was solved by heavy-atom methods and refined as a full matrix in least-squares calculations.[20] Hydrogen atoms were placed in observed positions and held invariant; their isotropic temperature parameters were all tied to a single variable. All non-hydrogen atoms were refined anisotropically. In a final cycle of least-squares refinement, the maximum shift was $<0.02\sigma$. No correction for secondary extinction was made. The highest peak on a final difference map represented 0.96 e Å$^{-3}$ in the vicinity of one of the Cu atoms. The number of observations was 3824, and the number of variable parameters was 317. Neutral-atom scattering factors and corrections for anomalous dispersion were from ref 21. Other details of the crystallographic experiment are given in Table II.

(18) Holm, R. H.; Patterson, G. S. *Inorg. Chem.* **1972**, *11*, 2285.
(19) DeMeulenear, I.; Tompa, H. *Acta Crystallogr.* **1965**, *19*, 1014.
(20) Computations were performed by using local modifications of the programs of SHELX-76: G. M. Sheldrick, University Chemical Laboratory, Cambridge, England, 1976.
(21) *International Tables for X-ray Crystallography*; Kynoch: Birmingham, England, 1974; Vol. 4.

**Table III.** Atomic Positional Parameters for $Cu_2(PAAet)_2 \cdot {}^1/_2C_6H_6$

| atom | $x$ | $y$ | $z$ |
|---|---|---|---|
| Cu1 | −0.02586 (4) | 0.13899 (3) | 0.65750 (4) |
| Cu2 | −0.11460 (4) | −0.08025 (3) | 0.71352 (4) |
| N1 | 0.1511 (3) | 0.1913 (2) | 0.6004 (2) |
| N2 | −0.2836 (3) | −0.1368 (2) | 0.7822 (2) |
| O1 | 0.0379 (2) | −0.0008 (2) | 0.6440 (2) |
| O2 | −0.0040 (3) | −0.2090 (2) | 0.7143 (2) |
| O3 | −0.1184 (3) | 0.2632 (2) | 0.6886 (2) |
| O4 | −0.1835 (2) | 0.0615 (2) | 0.7188 (2) |
| C1 | 0.1730 (4) | 0.2944 (2) | 0.6174 (3) |
| C2 | 0.2515 (5) | 0.2846 (3) | 0.7355 (4) |
| C3 | 0.2532 (4) | 0.1377 (2) | 0.5535 (3) |
| C4 | 0.3883 (4) | 0.1825 (3) | 0.5102 (4) |
| C5 | 0.2516 (4) | 0.0340 (3) | 0.5434 (3) |
| C6 | 0.1577 (4) | −0.0344 (2) | 0.5955 (3) |
| C7 | 0.1904 (4) | −0.1434 (2) | 0.6006 (3) |
| C8 | 0.1189 (4) | −0.2222 (2) | 0.6637 (3) |
| C9 | 0.1826 (4) | −0.3374 (2) | 0.6842 (3) |
| C10 | 0.3226 (5) | −0.3553 (3) | 0.6211 (4) |
| C11 | 0.0764 (5) | −0.3952 (3) | 0.6370 (4) |
| C12 | 0.2080 (6) | −0.3803 (3) | 0.8198 (4) |
| C13 | −0.2849 (4) | −0.2508 (3) | 0.8006 (3) |
| C14 | −0.2305 (6) | −0.3107 (3) | 0.9248 (4) |
| C15 | −0.3943 (4) | −0.0802 (3) | 0.8152 (3) |
| C16 | −0.5277 (5) | −0.1269 (3) | 0.8629 (4) |
| C17 | −0.4023 (4) | 0.0280 (3) | 0.8092 (4) |
| C18 | −0.3026 (4) | 0.0950 (2) | 0.7681 (3) |
| C19 | −0.3259 (4) | 0.1999 (3) | 0.7799 (3) |
| C20 | −0.2371 (4) | 0.2742 (2) | 0.7453 (3) |
| C21 | −0.2680 (4) | 0.3820 (2) | 0.7750 (3) |
| C22 | −0.4022 (5) | 0.3951 (3) | 0.8474 (4) |
| C23 | −0.2833 (5) | 0.4669 (3) | 0.6571 (4) |
| C24 | −0.1392 (5) | 0.3945 (3) | 0.8484 (4) |
| C25 | −0.1186 (5) | −0.0272 (4) | 1.0600 (4) |
| C26 | −0.0316 (5) | −0.0984 (3) | 1.0178 (4) |
| C27 | 0.0881 (5) | −0.0731 (4) | 0.9562 (4) |

**$Cu_2(PAApr)_2$.** The compound typically crystallized as deep green, nearly black, rectangular needles. A single crystal on a Nicolet R3 automated diffractometer equipped with Mo $K\alpha$ radiation and a graphite monochromator was used for data collection. Gaussian integration absorption corrections were applied. The structure was solved by heavy-atom methods and refined as a full matrix in least-squares calculations.[20] Hydrogen atoms were placed in observed positions and their positions refined; their isotropic temperature factors were all tied to a single variable. All non-hydrogen atoms were refined anisotropically. In a final cycle of least-squares refinement, the maximum shift was $0.1\sigma$ for non-hydrogen atoms. No correction for secondary extinction was made. The highest peak on a final difference map was 0.28e Å$^{-3}$. The number of observations was 1771, and the number of variable parameters was 218. Neutral-atom scattering factors and corrections for anomalous dispersion were from ref 21. Other details are given in Table II.

## Results

**1. Structure of $Cu_2(PAAet)_2 \cdot {}^1/_2C_6H_6$.** Final atomic coordinates, bond lengths, and bond angles for bis[2,2-dimethyl-7-(ethylimino)-3,5-octanedionato]dicopper(II)–$^1/_2$-benzene are given in Tables III and IV. The atomic labeling scheme is shown as follows:

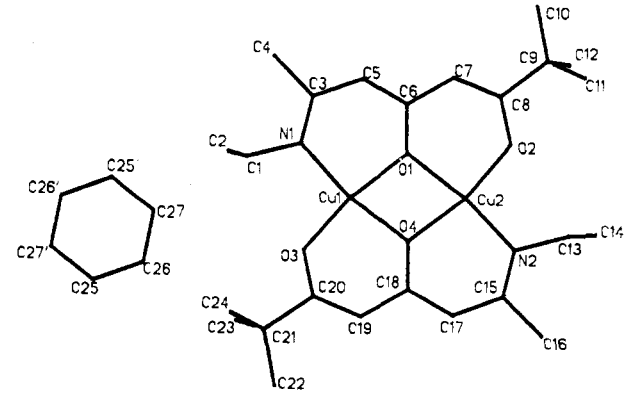


Although all atoms occupy general positions in the unit cell, the

**Table IV.** Bond Lengths (Å) and Angles (deg) for $Cu_2(PAAet)_2 \cdot {}^1/_2C_6H_6$

| | | | |
|---|---|---|---|
| Cu1–N1 | 1.942 (3) | C6–C7 | 1.430 (5) |
| Cu1–O1 | 1.923 (2) | C7–C8 | 1.373 (5) |
| Cu1–O3 | 1.878 (3) | C8–C9 | 1.533 (5) |
| Cu1–O4 | 1.952 (2) | C9–C10 | 1.520 (6) |
| Cu2–N2 | 1.934 (3) | C9–C11 | 1.518 (6) |
| Cu2–O1 | 1.948 (2) | C9–C12 | 1.516 (7) |
| Cu2–O2 | 1.883 (3) | C13–C14 | 1.497 (7) |
| Cu2–O4 | 1.929 (2) | C15–C16 | 1.517 (6) |
| N1–C1 | 1.475 (5) | C15–C17 | 1.417 (6) |
| N1–C3 | 1.313 (5) | C17–C18 | 1.384 (5) |
| N2–C13 | 1.482 (5) | C18–C19 | 1.425 (5) |
| N2–C15 | 1.314 (5) | C19–C20 | 1.364 (5) |
| O1–C6 | 1.328 (4) | C20–C21 | 1.546 (5) |
| O2–C8 | 1.302 (5) | C21–C22 | 1.522 (6) |
| O3–C20 | 1.299 (5) | C21–C23 | 1.519 (6) |
| O4–C18 | 1.327 (4) | C21–C24 | 1.529 (7) |
| C1–C2 | 1.506 (7) | C25–C26 | 1.348 (8) |
| C3–C4 | 1.508 (5) | C25–C27′ | 1.372 (8) |
| C3–C5 | 1.416 (5) | C26–C27 | 1.363 (7) |
| C5–C6 | 1.382 (5) | | |
| Cu1–N1–C1 | 117.3 (2) | O1–Cu2–O4 | 75.6 (1) |
| Cu1–N1–C3 | 123.4 (2) | O1–C6–C5 | 120.8 (3) |
| Cu1–O1–Cu2 | 104.5 (1) | O1–C6–C7 | 119.0 (3) |
| Cu1–O6–C6 | 127.4 (2) | O2–Cu2–O4 | 166.1 (1) |
| Cu1–O3–C20 | 126.7 (2) | O2–C8–C7 | 125.3 (3) |
| Cu1–O4–Cu2 | 104.1 (1) | O2–C8–C9 | 113.3 (3) |
| Cu1–O4–C18 | 128.0 (2) | O3–Cu1–O4 | 92.8 (1) |
| Cu2–N2–C13 | 117.3 (2) | O3–C20–C19 | 125.5 (4) |
| Cu2–N2–C15 | 123.5 (3) | O3–C20–C21 | 112.7 (3) |
| Cu2–O1–C6 | 128.2 (2) | O4–C18–C17 | 120.1 (3) |
| Cu2–O2–C8 | 126.5 (2) | O4–C18–C19 | 119.5 (3) |
| Cu2–O4–C18 | 127.4 (2) | C1–N1–C3 | 119.2 (3) |
| N1–Cu1–O1 | 94.3 (1) | C3–C5–C6 | 127.6 (4) |
| N1–Cu1–O3 | 97.1 (1) | C4–C3–C5 | 114.1 (3) |
| N1–Cu1–O4 | 169.6 (1) | C5–C6–C7 | 120.2 (3) |
| N1–C1–C2 | 111.6 (3) | C6–C7–C8 | 126.7 (4) |
| N1–C3–C4 | 121.1 (3) | C7–C8–C9 | 121.4 (3) |
| N1–C3–C5 | 124.8 (3) | C8–C9–C10 | 114.3 (3) |
| N2–Cu2–O1 | 170.5 (1) | C8–C9–C11 | 108.9 (3) |
| N2–Cu2–O2 | 96.8 (1) | C8–C9–C12 | 106.8 (4) |
| N2–Cu2–O4 | 95.0 (1) | C10–C9–C11 | 107.4 (4) |
| N2–C13–C14 | 111.9 (4) | C10–C9–C12 | 108.8 (4) |
| N2–C15–C16 | 121.7 (4) | C11–C9–C12 | 110.5 (4) |
| N2–C15–C17 | 124.4 (4) | C13–N2–C15 | 119.1 (3) |
| O1–Cu1–O3 | 168.3 (1) | C15–C17–C18 | 129.1 (4) |
| O1–Cu1–O4 | 75.7 (1) | C16–C15–C17 | 113.9 (4) |
| O1–Cu2–O2 | 92.6 (1) | C17–C18–C19 | 120.4 (3) |
| C18–C19–C20 | 127.0 (3) | C22–C21–C23 | 108.6 (4) |
| C19–C20–C21 | 121.8 (3) | C22–C21–C24 | 108.8 (4) |
| C20–C21–C22 | 113.9 (3) | C23–C21–C24 | 109.1 (4) |
| C20–C21–C23 | 108.9 (4) | C25–C26–C27 | 121.4 (5) |
| C20–C21–C24 | 107.3 (3) | C26–C25–C27′ | 120.9 (5) |

center of the benzene molecule lies on a crystallographic inversion center. The packing in the lattice (see Figure 1) is composed of identical stacks of repeating units of copper complex/benzene/copper complex sandwiches forming an ADAADA... arrangement where A is the metal chelate and D represents a benzene molecule. Since the benzene occupies an inversion center, it is necessarily equidistant between the two chelate molecules. Within an ADA unit, the substituents on the chelates are mutually oriented in such a way that they encapsulate the benzene molecule (see Figure 2). Although there are significant deviations from planarity, a best plane can be calculated through the entire copper chelate complex, minus the substituents (Table V, plane no. 3). The distance from this plane to the centroid of the benzene ring is 3.390 Å, corresponding to the A–D distance in the ADAADA... stack. The dihedral angle between the best plane through the copper chelate (minus substituents) and the plane of the encapsulated benzene is 7.2°. The degree of tilt within a stack can be described as the angle between the vector of stacking and the plane of the benzene molecule and is 55.6 (5)°.

The overlap diagram shown in Figure 3 views an A–D pair perpendicular to the plane of the benzene. As is shown, the

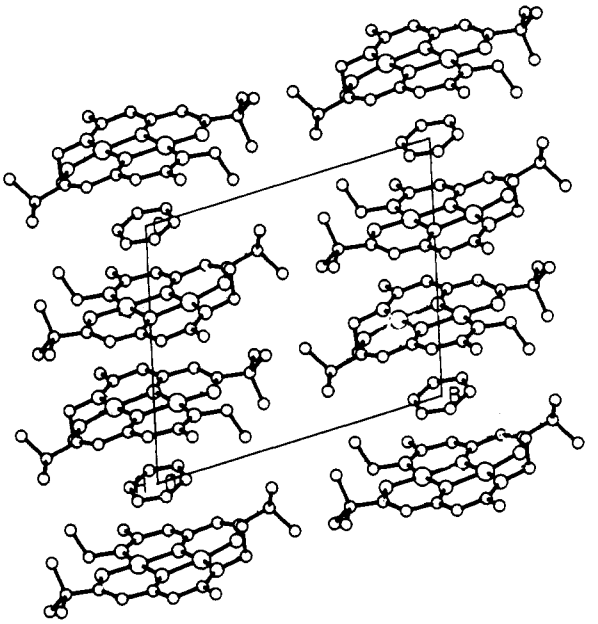

**Figure 1.** Unit cell packing diagram for $Cu_2(PAAet)_2 \cdot {}^1/_2C_6H_6$ viewed along the *a* crystallographic axis. The complex and solvent form stacks of an ADAADA... pattern.

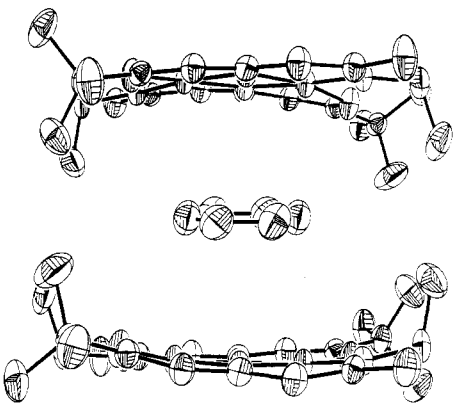

**Figure 2.** Diagram of a single ADA unit of $Cu_2(PAAet)_2 \cdot {}^1/_2C_6H_6$, showing the encapsulation of the solvent molecule. Thermal ellipsoids represent 50% probability.

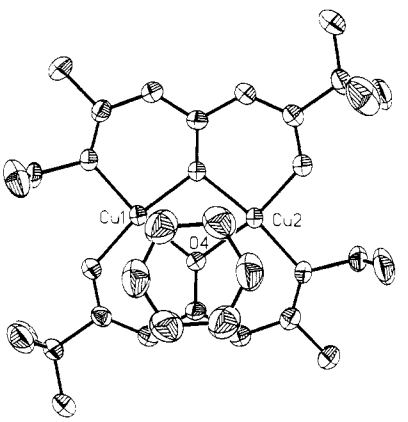


**Figure 3.** Overlap diagram of $Cu_2(PAAet)_2 \cdot {}^1/_2C_6H_6$. The copper complex is projected onto the plane of the benzene molecule and viewed perpendicular to it. Thermal ellipsoids represent 50% probability.

benzene interaction is not centered on the $Cu_2O_2$ portion of the molecule, as it was in the related complexes $Cu_2(PAAan)_2 \cdot C_6H_6$ and $Cu_2(PAApnan)_2 \cdot C_6H_6$. Rather, it is displaced to the side so that atom O4 (a bridging oxygen atom) is roughly centered in the projection of the $Cu_2(PAAet)_2$ molecule on the benzene both

**Table V.** Least-Squares Planes and Displacements (Å) for $Cu_2(PAAet)_2 \cdot {}^1/_2C_6H_6$

Plane No. 1: Donor Atoms around Cu1; Defined by Atoms N1, O1, O3, O4 (RMSD = 0.007 Å)

| | | | | | |
|---|---|---|---|---|---|
| N1 | −0.006 | O3 | 0.006 | Cu1 | 0.044 |
| O1 | −0.006 | O4 | −0.007 | Cu2 | −0.145 |

Plane No. 2: Donor Atoms around Cu2; Defined by Atoms N2, O1, O2, O4 (RMSD = 0.064 Å)

$-3.537x - 2.210y - 10.496z = -6.962$

| | | | | | |
|---|---|---|---|---|---|
| N2 | 0.057 | O2 | −0.059 | Cu2 | 0.056 |
| O1 | 0.071 | O4 | −0.069 | Cu1 | −0.155 |

Plane No. 3: Entire Binuclear Molecule minus Substituent; Defined by Atoms Cu1, Cu2, N1, N2, O1–O4, C3, C5–C8, C15, C17–C20 (RMSD = 0.126 Å)

$-3.903x - 1.005y - 10.121z = -6.730$

| | | | | | |
|---|---|---|---|---|---|
| Cu1 | 0.037 | O4 | 0.110 | C17 | 0.083 |
| Cu2 | 0.037 | C3 | 0.002 | C18 | 0.042 |
| N1 | −0.128 | C5 | 0.214 | C19 | −0.092 |
| N2 | 0.058 | C6 | 0.122 | C20 | −0.163 |
| O1 | 0.066 | C7 | 0.053 | Ctd[a] | −3.390 |
| O2 | −0.273 | C8 | −0.228 | Cen[b] | 3.278 |
| O3 | −0.041 | C15 | 0.099 | | |

Plane No. 4: Benzene Ring; Defined by Atoms C25–C27

$-4.773x - 0.261y - 9.392z = -9.382$

Dihedral Angles (deg) between Calculated Planes: 1–2 = 8.1 (3); 3–4 = 7.2 (1.2)

[a] Ctd is defined as the centroid of the benzene ring. [b] Cen is defined as the center of the Cu1, Cu2, O1, O4 ring of an adjacently stacked molecule.

**Table VI.** Atomic Positional Parameters for $Cu_2(PAApr)_2$

| atom | x | y | z |
|---|---|---|---|
| Cu1 | 0.05470 (3) | 0.16890 (6) | 0.05137 (2) |
| O1 | 0.2078 (2) | 0.1866 (4) | 0.0969 (1) |
| O2 | 0.0923 (2) | −0.0883 (4) | −0.0006 (1) |
| N1 | 0.0082 (2) | −0.4222 (4) | −0.0926 (1) |
| C1 | 0.3891 (4) | 0.1371 (9) | 0.2046 (2) |
| C2 | 0.4438 (4) | 0.3607 (7) | 0.1054 (3) |
| C3 | 0.5197 (3) | −0.0135 (7) | 0.1181 (2) |
| C4 | 0.4130 (3) | 0.1336 (5) | 0.1280 (2) |
| C5 | 0.2989 (3) | 0.0656 (5) | 0.0855 (2) |
| C6 | 0.2965 (3) | −0.1040 (5) | 0.0404 (2) |
| C7 | 0.1982 (3) | −0.1858 (5) | −0.0022 (1) |
| C8 | 0.2089 (3) | −0.3645 (6) | −0.0426 (2) |
| C9 | 0.1223 (3) | −0.4770 (5) | −0.0843 (1) |
| C10 | 0.1676 (4) | −0.6721 (7) | −0.1201 (2) |
| C11 | −0.0756 (3) | −0.5598 (6) | −0.1342 (2) |
| C12 | −0.0894 (4) | −0.5003 (7) | −0.2114 (2) |
| C13 | −0.1809 (4) | −0.6404 (9) | −0.2508 (3) |

above and below the benzene plane. The perpendicular distance between O4 and the benzene plane is 3.491 Å. The proximity of the benzene to half the $Cu_2(PAAet)_2$ molecule creates a nonequivalency in the halves of the molecule. However no significant ($>3\sigma$) differences in bond lengths or angles can be found between the two chelate ligands.

The copper atoms are four-coordinate and are displaced only slightly (0.04 and 0.06 Å) out of the best plane of their respective donor atoms. The two coordination planes are inclined 8.1° with respect to each other, following the slight curvature of the molecule evident in Figure 2.

The two copper chelate molecules that are adjacently stacked have 3.278 Å between the mean plane of the one molecule and the center of the molecule stacked adjacently, corresponding to the A–A distance in the ADAADA... stack. When one views the A–A molecules as a projection on the plane of the central atoms (Cu1, Cu2 and O1), it is evident that Cu2 eclipses the atom C5 in an adjacent molecule. Indeed, the closest intermolecular contact to Cu exists at this point with a distance of 3.090 Å between Cu2 and C5′. This distance is just the sum of the van der Waals radii for Cu and C.[22]

**Table VII.** Bond Lengths (Å) and Angles (deg) for $Cu_2(PAApr)_2$

| | | | |
|---|---|---|---|
| Cu1–O1 | 1.877 (2) | C3–C4 | 1.538 (5) |
| Cu1–O2 | 1.957 (2) | C4–C5 | 1.530 (4) |
| Cu1–O2′ | 1.925 (2) | C5–C6 | 1.369 (4) |
| Cu1–N1′ | 1.930 (3) | C6–C7 | 1.421 (4) |
| O1–C5 | 1.308 (4) | C7–C8 | 1.370 (4) |
| O2–C7 | 1.343 (4) | C8–C9 | 1.403 (5) |
| N1–C9 | 1.330 (4) | C9–C10 | 1.508 (5) |
| N1–C11 | 1.468 (4) | C11–C12 | 1.528 (4) |
| C1–C4 | 1.517 (5) | C12–C13 | 1.511 (6) |
| C2–C4 | 1.532 (5) | Cu1···Cu1′ | 3.083 (1) |
| Cu1–O1–C5 | 126.5 (2) | N1–C9–C10 | 120.8 (3) |
| Cu1–O2–C7 | 127.8 (2) | N1–C11–C12 | 113.6 (3) |
| Cu1–O2′–C7′ | 127.0 (2) | C1–C4–C2 | 108.9 (3) |
| Cu1–N1′–C9′ | 123.0 (2) | C1–C4–C3 | 109.2 (3) |
| Cu1–N1′–C11′ | 117.6 (2) | C1–C4–C5 | 108.5 (3) |
| O1–Cu1–O2 | 93.35 (9) | C2–C4–C3 | 108.8 (3) |
| O1–Cu1–O2′ | 167.6 (1) | C2–C4–C5 | 107.7 (3) |
| O1–Cu1–N1′ | 96.6 (1) | C3–C4–C5 | 113.6 (3) |
| O1–C5–C4 | 112.9 (3) | C4–C5–C6 | 121.9 (3) |
| O1–C5–C6 | 125.1 (3) | C5–C6–C7 | 128.4 (3) |
| O2–Cu1–O2′ | 74.83 (9) | C6–C7–C8 | 121.4 (3) |
| O2–Cu1–N1′ | 170.0 (1) | C7–C8–C9 | 130.1 (3) |
| O2–C7–C6 | 118.5 (3) | C8–C9–C10 | 114.9 (3) |
| O2–C7–C8 | 120.0 (3) | C9–N1–C11 | 119.4 (3) |
| O2′–Cu1–N1′ | 95.4 (1) | C11–C12–C13 | 111.1 (3) |
| N1–C9–C8 | 124.3 (3) | Cu1–O2–Cu1′ | 105.2 (1) |

**Table VIII.** Least-Squares Planes and Displacements (Å) for $Cu_2(PAApr)_2$

Plane No. 1 Donor Atoms around Cu; Defined by Atoms O1, O2, O2′, N1′ (RMSD = 0.043 Å)

$3.733x + 3.477y - 15.113z = 0.0$

| | | | | | |
|---|---|---|---|---|---|
| O1 | −0.039 | O2′ | −0.046 | Cu | 0.016 |
| O2 | 0.047 | N1′ | 0.039 | | |

Plane No. 2 Entire Molecule minus Substituents; Defined by atoms Cu, O1, O2, N1, C4–C11 (RMSD = 0.067 Å)

$3.149x + 3.596y - 15.161z = -0.078$

| | | | | | |
|---|---|---|---|---|---|
| Cu | 0.079 | C4 | −0.082 | C8 | 0.070 |
| O1 | −0.066 | C5 | −0.041 | C9 | 0.026 |
| O2 | 0.060 | C6 | 0.026 | C10 | 0.009 |
| N1 | −0.011 | C7 | 0.068 | C11 | −0.139 |

**Table IX.** Selected Structural Comparisons (Å)

| | ref | intramolecular Cu···Cu | A–D stack dist | adjacent A–A stack dist | Cu–O–(trans N) |
|---|---|---|---|---|---|
| complex·$2C_6H_6$ | 14 | 3.030 (1) | 3.262 (8)[a] | | 1.931 (2) |
| complex·$1C_6H_6$ | 14 | 3.046 (2) | 3.258 (2)[a] | | 1.946 (3) |
| complex·$0.5C_6H_6$ | *d* | 3.060 (1) | 3.390 (5)[b] | 3.278 (5)[c] | 1.948 (2) 1.952 (2) |
| complex·$0C_6H_6$ | *d* | 3.083 (1) | | 3.477 (2)[c] | 1.957 (2) |

[a] Distance between centers calculated by mean positions. [b] Distance between complex best plane and the benzene centroid. [c] Perpendicular distance between complex center (average Cu1, Cu2, O1, O4 positions) and the best plane of the adjacent stacked complex. [d] This work.

In the solvent benzene molecule, the C–C bond distances are not equivalent and vary 1.348–1.372 Å ($7\sigma$ range). The mean value is 1.361 (12) Å. The atomic geometry within the ketonate complex is normal[23–25].

**2. $Cu_2(PAApr)_2$.** Tabular data for bis[2,2-dimethyl-7-(*n*-propylimino)-3,5-octanedionato]dicopper(II) are presented in Tables VI–VIII and include fractional atomic coordinates, bond

(22) van der Waals radii for Cu (1.4 Å) and for C (1.65–1.7 Å) are collected in: Huheey, J. E. *Inorganic Chemistry*; Harper and Row: New York, 1972; p 184.
(23) Lintvedt, R. L.; Glick, M. D.; Tomlonovic, B. K.; Gavel, D. P.; Kuszaj, J. M. *Inorg. Chem.* **1976**, *15*, 1633.
(24) Blake, A. B.; Fraser, L. R. *J. Chem. Soc., Dalton Trans.* **1974**, 2554.
(25) Heeg, M. J.; Mack, J. L.; Glick, M. D.; Lintvedt, R. L. *Inorg. Chem.* **1981**, *20*, 833.

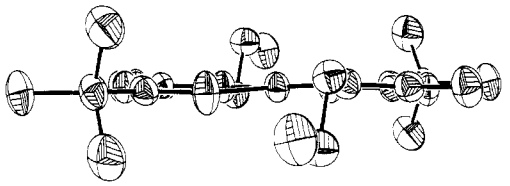

**Figure 4.** Side-on view of $Cu_2(PAApr)_2$ illustrating its planarity. Thermal ellipsoids represent 50% probability.

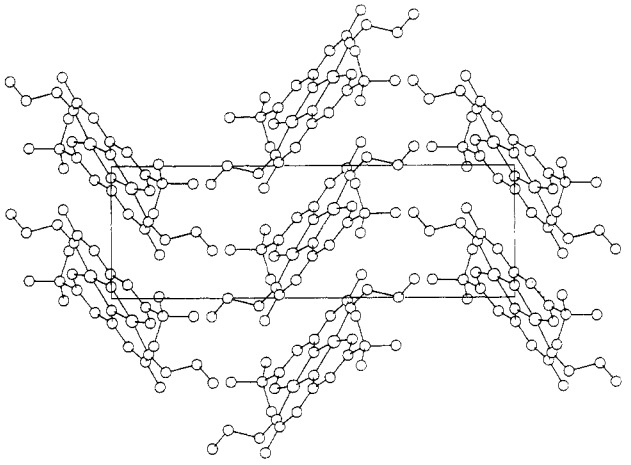

**Figure 5.** Packing diagram of $Cu_2(PAApr)_2$ viewed along the *a* crystallographic axis.

**Table X.** UV–Visible Data for Selected Bis[2,2-dimethyl-7-(R-imino)-3,5-octanedionato]dicopper(II) Complexes[a]

| R | $\lambda_{max}$, nm | | |
|---|---|---|---|
| | $CHCl_3$ | $C_7H_8$ | DMF |
| $CH_3$ | 604 (326) | 609 (293) | 615 (276) |
| $CH_3CH_2$ | 607 (302) | 611 (265) | 616 (256) |
| $C_6H_5$ | 609 (368) | 614 (346) | 628 (328) |
| $p$-$C_6H_4CH_3$ | 609 (450) | 614 (333) | 639 (286) |
| $p$-$C_6H_4NO_2$ | 608 (464) | 615 (403) | 639 (324) |
| $p$-$C_6H_4Cl$ | 610 (429) | 614 (418) | 634 (346) |
| $p$-$C_6H_4Br$ | 608 (389) | 613 (366) | 634 (334) |
| $p$-$C_6H_4CF_3$ | 610 (394) | 616 (296) | 639 (334) |

[a] Extinction coefficient in parentheses. Temperature 23 ± 2 °C, λ ± 2 nm, and ε ± 3.

lengths and bond angles, and least-squares planes. Labeling is given as follows:

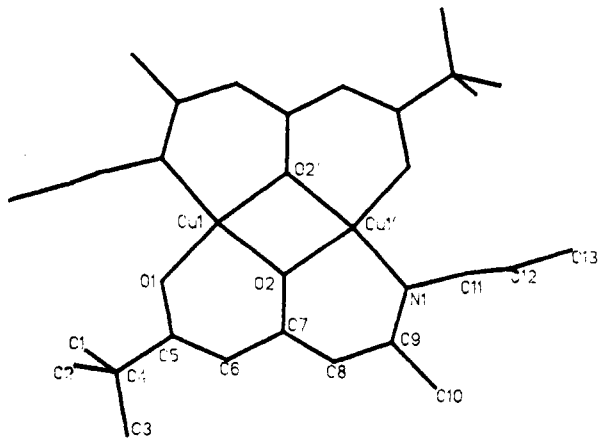


Figures 4 and 5 illustrate the molecular geometry and packing. All atoms are located on general positions, but the molecular center occupies a crystallographic inversion center so that there is one-half molecule per asymmetric unit.

The copper atom is four-coordinate and only 0.016 Å out of the best plane through its donor ligands. The closest intermolecular axial contact to Cu is to C9′ at a distance of 3.55 Å. The perpendicular distance from the center of the molecule to the best plane of an adjacent molecule is 3.477 Å. The ligand geometry is normal.

**Table XI.** $^1H$ NMR Resonances for Bis[2,2-dimethyl-7-(R-imino)-3,5-octanedionato]dicopper(II) Complexes[a]

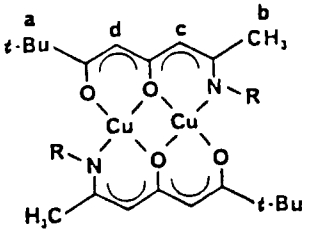


| substituent | *a* | *b* | *c*, *d* | R |
|---|---|---|---|---|
| $CH_3$ | 1.09 | 1.48 | 5.05 | |
| $CH_3CH_2$ | 1.06 | 1.47 | 4.97 | 0.94 ($CH_3$) |
| $n$-$C_3H_7$ | 1.06 | 1.47 | 4.94 | 0.89 ($CH_3$) |
| | | | 5.17 | 1.40 |
| | | | | 1.71 ($CH_2$) |
| $n$-$C_4H_9$ | 1.06 | 1.49 | 4.94 | 0.91 ($CH_3$) |
| | | | 5.16 | 1.33 ($CH_2$) |
| $C_6H_5$ | 0.63 | 1.21 | 5.11 | 6.39 |
| | | | 5.20 | 6.56 |
| | | | | 7.41 |
| $p$-$C_6H_4CH_3$ | 0.64 | 1.21 | 5.07 | 2.71 (PhC$H_3$) |
| | | | 5.19 | 6.26 |
| | | | | 7.41 (Ph) |
| $p$-$C_6H_4OCH_3$ | 0.66 | 1.22 | 5.06 | 3.78 (PhOC$H_3$) |
| | | | 5.19 | 6.30 |
| | | | | 6.94 (Ph) |
| $p$-$C_6H_4Cl$ | 0.67 | 1.25 | 5.11 | 6.35 |
| | | | 5.21 | 7.39 (Ph) |
| $p$-$C_6H_4Br$ | 0.67 | 1.23 | 5.13 | 6.27 |
| | | | 5.23 | 7.54 (Ph) |
| $p$-$C_6H_4NO_2$ | 0.62 | 1.30 | 5.23 | 6.57 |
| | | | 5.28 | 8.34 (Ph) |
| $p$-$C_6H_4CF_3$ | 0.61 | 1.27 | 5.16 | 6.53 |
| | | | 5.24 | 7.41 (Ph) |

[a] Shifts relative to chloroform (7.26 ppm).

**Absorption Spectra.** The binuclear complexes all exhibit two bands in the UV–visible region of the spectrum. The d–d band is observed between 604 and 639 nm, depending upon the solvent. This solvent dependency is summarized in Table X. In general, as the basicity (coordinating ability) increases, the band is shifted to lower energy. The energy of the band maximum does not appear to be much affected by changes in the nitrogen substituent. A higher energy band, which appears to be a shoulder of a more intense band at shorter wavelength, is centered at about 430 nm with an extinction coefficient of about $4 \times 10^3$ L mol$^{-1}$ cm$^{-1}$. The wavelength and extinction coefficients are reasonably independent of changes in the solvent or substituent.

**Nuclear Magnetic Resonance.** $^1H$ NMR spectra of the complexes were examined over the −6.0 to +16.0 ppm range, and the results are summarized in Table XI. There are several features of this data that are significant. First, to our knowledge these are the first high-resolution $^1H$ spectra recorded for copper(II) complexes. These complexes exhibit very strong antiferromagnetic exchange. Indeed, Faraday method magnetic susceptibility measurements indicate they are diamagnetic at room temperature.[14] As a result, NMR spectra can be obtained. The line widths are only slightly broadened, varying from 6 to 24 Hz, indicative of very low residual paramagnetism.

Second, the protons adjacent ($\alpha$) to the nitrogen atom are strongly shielded by the copper center. When R is an alkyl group, the $\alpha$ proton is located near $\delta$ 3.2 in the NMR spectra of the enolized Schiff bases. Upon complexation this proton peak shifts upfield to about $\delta$ 1.0.

Third, there is a significant difference in the *tert*-butyl resonance (and the ketimine methyl resonance), depending upon whether

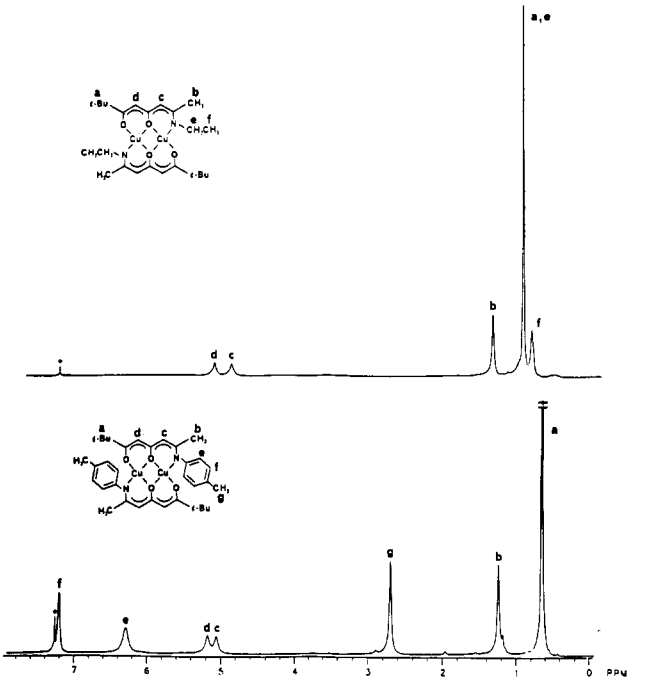


**Figure 6.** Proton resonance spectra of $Cu_2(PAAea)_2$ (top) and $Cu_2$-$(PAA/p\text{-methyl})_2$ (bottom) in $CDCl_3$ at 300 MHz and 25 °C.

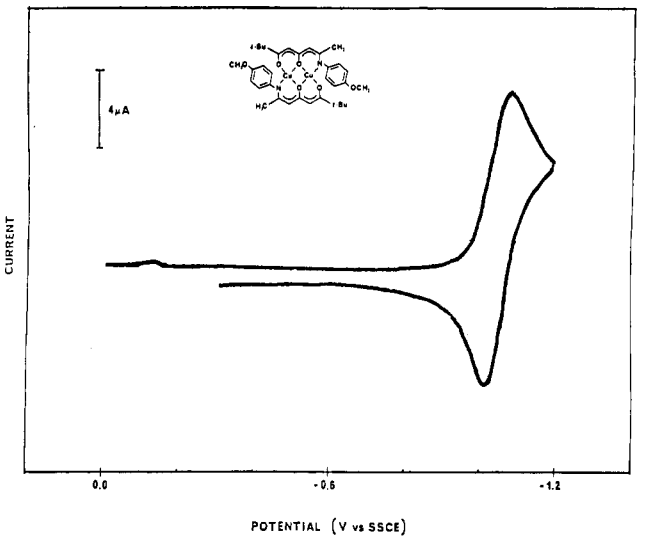


**Figure 7.** Cyclic voltammogram of $Cu_2(PAA/p\text{-methoxy})_2$ in a 0.10 M TEAP–DMF solution from 0.00 to −1.20 V vs SSCE (sweep rate 200 mV/s).

the R substituent is aromatic or aliphatic. This is illustrated in Figure 6. A plausible explanation for this is that when the *tert*-butyl group is exposed to the anisotropy generated by an aromatic ring, the group is shielded and an upfield shift is observed. This phenomenon is also present for the ketimine methyl resonance, but to a lesser degree.

**Electrochemistry.** Electrochemical measurements were performed on $10^{-3}$–$10^{-4}$ M solutions of the complexes in DMF. For direct comparison of the values obtained, the conditions under which the experiments were performed were kept as constant as possible throughout the entire series of complexes. Figure 7 shows the typical voltammetric response for these complexes in the potential region of interest. The voltammogram was essentially the same for all the complexes, independent of the scan rate (50–1000 mV/s). For the most part, $\Delta E_p$, $E_p - E_{pc}/2$, and $I_{pc}/v^{1/2}$ are constant as a function of scan rate and indicative of a one-electron, reversible system.[26] Expansion of the potential window

(26) Shain, I.; Poycyn, D. S. *Anal. Chem.* **1966**, *38*, 370.

**Table XII.** Redox Properties for Bis[2,2-dimethyl-7-((4-X-phenyl)imino)-3,5-diketonato]dicopper(II) Complexes[a]

| X | $E_{1/2}$[b] | $\Delta E_p$ | $2\sigma_p$[c] |
|---|---|---|---|
| $OCH_3$ | −1.05 | 54 | −0.54 |
| $CH_3$ | −1.03 | 68 | −0.34 |
| H | −1.02 | 66 | 0.0 |
| Cl | −0.98 | 59 | 0.46 |
| Br | −0.98 | 74 | 0.46 |
| $NO_2$ | −0.88 | 72 | 1.56 |

[a] 0.10 M TEAP/DMF solutions; temperature 23 ± 2 °C. [b] Volts vs SSCE, ±0.01 V. [c] $\sigma_p$ values from: Zuman, P. *Substituent Effects in Organic Polarography*; Plenum: New York, p 46.

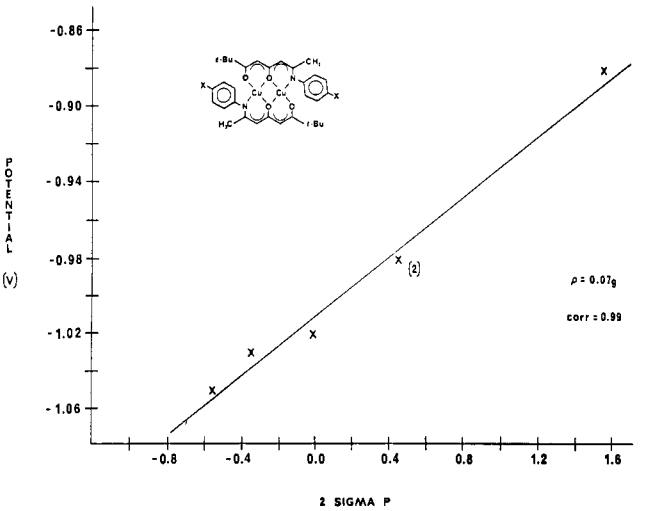


**Figure 8.** Hammett plot of $E_{1/2}$ vs $2\sigma_p$ (correlation 0.99, slope 0.08) illustrating the dependence of redox potentials on $\sigma_p$. The substituent $2\sigma_p$ values are given in Table XII.

to −2.0 V shows an irreversible wave at −1.5 V associated with the second Cu(II) to Cu(I) reduction.

The electrochemical data for the series (R = $OCH_3$, $CH_3$, H, Cl, Br, $NO_2$) are given in Table XII. Potentials are listed as $E_{1/2}$ values for the reversible reduction. The series contains Schiff-base complexes with various electron-donor and -withdrawing groups that have different Hammett ($\sigma_p$) values. In general, as the electron-donating ability of the substituent increases, the observed potential shifts in the cathodic direction. A plot of $E_{1/2}$ versus $2\sigma_p$ is linear, as shown in Figure 8, with a correlation coefficient of 0.99 and $\rho = 0.079$.

## Discussion

Table XII shows the $E_{1/2}$ values obtained for voltammograms for the first metal reduction. As the electron-donating power of the substituent group is increased, the $Cu^{2+}/Cu^{1+}$ reduction becomes more difficult. This implies that the substituent group directly affects the electron density on the metal atoms. With an increase in the electron-donating power of the substituent groups, more electron density resides on the chelate ring, which would in turn result in more electron density on the metal atoms. The greater the electron density present on the metal atoms as the result of electronic properties of the substituent groups, the more difficult it should be to perform the reduction. This is exactly the behavior that is observed.

To quantify the observed variation, the dependence of the reduction potential on the substituent groups was correlated to the Hammett substituent constants.[27] Figure 8 shows the first reduction potential versus the $2\sigma_p$ constant for the copper/PAA/aromatic imine series. The observed linear correlation is quite useful since this type of relationship readily allows extrapolation and interpolation of the $Cu^{2+}/Cu^{1+}$ reduction potential.

(27) Gordon, A. J.; Ford, R. A. *The Chemists Companion*; Wiley: New York, 1972; pp 144–153. Zuman, P. *Substituent Effects in Organic Polarography*; Plenum: New York, 1967; p 46.

It is interesting to compare the effects of substituents in these complexes with those observed in porphyrins, macrocycles, and other Schiff-base complexes. Kadish,[28] Walker,[29] and Meyer[30] have examined remote-substituent effects in porphyrin complexes by substituting various groups at the para position of the phenyl rings of tetraphenylporphyrins. The reaction constant, $\rho$, obtained was between 0.030 and 0.040 for the metal-based redox potential. Examining the $Ni^{2+}/Ni^{3+}$ oxidation potentials, Busch[31] obtained reaction constants of 0.035, 0.064, and 0.047 for a series of 14-, 15-, and 16-membered-ring tetraaza macrocycles, respectively, with para-substituted benzoyl groups in the $\gamma$ and $\gamma'$ positions. Addison[32] calculated a $\rho$ value of 0.076 based on the $Cu^{2+}/Cu^{1+}$ reduction in a series of pyrrole-2-carboxaldimate complexes. For the Schiff bases reported in this work, the $\rho$ value of 0.079 is comparable to those cited above. In all of these complexes the substituent is five to eight bonds from the redox site.

In the electronic spectra the d–d transition does not appear to be affected by the substituent group of the Schiff-base ligands. However, there is a bathochromic shift in this band (Table X) as the coordinating ability of the solvent is increased. The site symmetry of the Cu(II) ion in the triketonates is essentially planar.[33] In basic solvents, the solvent molecules exert a $z$-component field, and thus the coordination may now be regarded as tetragonally distorted. There are three d–d electronic transitions in a tetragonal complex—two of which contain a $z$ component and therefore would be affected by axial coordination. The three transitions, $\nu_1$, $\nu_2$, and $\nu_3$, shift in such a fashion that an overall decrease in frequency would be expected as the basicity of the solvent increases.[34] From Table X we see that, indeed, the d–d transition maximum shifts some 30 nm to a longer wavelength as the solvent changes from chloroform to *N,N*-dimethylformamide.

All of the Cu(II) complexes of the Schiff-base ligands exhibit an intense band centered at about 360 nm ($\epsilon_{max}$ 15 000–20 000). The major component of the band is assigned as a $\pi$ to $\pi^*$ transition involving delocalization throughout the azomethine chromophore. The band centered at about 430 nm appears to be a shoulder of the more intense band at shorter wavelength and may be attributed to a d to $\pi^*$ charge-transfer transition. These assignments would be consistent with those of Waters and Wright[35] for (salicylaldimine)copper(II) complexes and other dicopper(II) complexes.[36]

There are many examples in the literature of proton magnetic resonance spectra of complexes containing a diamagnetic Cu(I) center.[37] Cu(II), however, has intrinsically different spectral properties compared to those of Cu(I). Indeed, because of its paramagnetism, broadening of signals occurs and proton magnetic resonance spectra are generally unattainable. The dinuclear Cu(II) Schiff-base compounds examined in this work exhibit strong antiferromagnetic exchange and within the error limits of the Faraday method appear diamagnetic at room temperature. This particular characteristic in this series of complexes has allowed us to generate proton magnetic resonance spectra with reasonably sharp peaks.

Examination of Table XI and Figure 6 shows appreciably different chemical shifts for the *tert*-butyl group resonance, which is dependent upon the R substituent of the ketimine moiety. If the R group is aromatic, the resonance is shifted 0.5 ppm upfield of the resonance observed when R is aliphatic. Molecular models indicate that the *tert*-butyl group is near the $\pi$ cloud of the adjacent phenyl group. This causes a diamagnetic shielding of the protons and an upfield shift in their resonance. Martell and McCarthy[38] have observed the same magnetic shielding effects in the nickel(II) chelate of bis(acetylacetone) stilbenediimine.

A general trend in chemical shifts is apparent when examining the neutral-ligand resonances versus the same resonances in various Cu(I) complexes. In a series of sulfhydryl- and imidazole-containing tripeptides, Suguira[39] has observed that upon complexation the $\alpha_1$ proton (adjacent to the sulfhydryl group) signal shifts downfield 0.57–0.78 ppm with the remaining protons of the tripeptide also shifting to lower field. Temussi and Vitagliano[40] noted that the protons of the imidazole ring in the Cu(I) complexes of acetylhistamine and acetyl-L-histidine were shifted 0.4–0.7 ppm downfield from the free-ligand peaks. In ternary complexes of Cu(I) with 2,9-dimethyl-1,10-phenanthroline, Kwik and Ang[41] recorded shifting of the aromatic protons from 0.24 to 0.56 ppm downfield of the resonance for the uncoordinated phenanthroline. The methyl groups, however, were shifted upfield 0.17–0.50 ppm. The direction of shift of these methyl protons is exactly the behavior observed for the reported Cu(II) Schiff-base complexes, but to a lesser degree. The protons $\alpha$ to the nitrogen atoms shift upfield 2.0 ppm for aliphatic substituents and 0.8 ppm for aromatic substituents. This unique chemical shifting is most likely an effect of the central metal's small residual paramagnetism.

The structures reported herein complete the examination of a series of benzene/copper ketimine compounds in which the ratios of benzene:copper ketimine are 2:1, 1:1, 0.5:1, and 0:1. The ketimine ligands in these four examples are 2,2-dimethyl-7-((4-nitrophenyl)imino)-3,5-octanedionate, 2,2-dimethyl-7-(phenylimino)-3,5-octanedionate, 2,2-dimethyl-7-(ethylimino)-3,5-octanedionate, and 2,2-dimethyl-7-(*n*-propylimino)-3,5-octanedionate, abbreviated PAApnan, PAAan, PAAet, and PAApr, respectively. These are closely related in that they vary only in the substituent at the nitrogen atoms. Table IX summarizes the important structural features for comparison.

$\pi$ complexes of porphyrins and metalloporphyrins have been known for some time[42] and have been the subject of a number of investigations.[43] The evidence for $\pi$-molecular interactions in these solvated crystals must be inferred given only this static view of the molecules. Each of the first three entries (Table IX) fit the generalized picture[44] of a $\pi$-molecular compound; they all form one-dimensional stacks of nearly parallel molecules with interplanar distances equal to those found in known $\pi$-molecular compounds. These points have previously been discussed.[14]

Within these particular compounds benzene acts as the $\pi$ donor while the copper–ketimine complex serves as the $\pi$ acceptor. This is in contrast to many examples wherein the metal complexes act as $\pi$ donors and not as $\pi$ acceptors.[45] $\pi$-Molecular complex models where the members are a metal compound and a $\pi$ donor

(28) Kadish, K. M.; Morrison, M. M.; Constant, L. A.; Dickens, L.; Davis, D. G. *J. Am. Chem. Soc.* **1976**, *98*, 8387.
(29) Walker, F. A.; Beroiz, D.; Kadish, K. M. *J. Am. Chem. Soc.* **1976**, *98*, 3484.
(30) Meyer, T. J.; Rillema, D. P.; Nagle, J. K.; Barringer, L. F. *J. Am. Chem. Soc.* 1981, *103*, 56.
(31) Busch, D. H.; Streeky, J. A.; Pillsbury, D. G. *Inorg. Chem.* **1980**, *19*, 3148.
(32) Addison, A. W.; Stenhouse, J. H. *Inorg. Chem.* **1978**, *17*, 2161.
(33) Lintvedt, R. L.; Glick, M. D.; Anderson, T. J.; Mack, J. L. *Inorg. Chem.* **1976**, *15*, 2258.
(34) Huheey, J. E. *Inorganic Chemistry—Principles of Structure and Reactivity*; Harper and Row: New York, 1978; pp 384–387.
(35) Waters, T. N.; Wright, P. E. *J. Inorg. Nucl. Chem.* **1971**, *33*, 359.
(36) Urbach, F. L.; Grzybowski, J. J.; Merrell, P. H. *Inorg. Chem.* **1978**, *17*, 3078. Urbach, F. L.; Downing, R. S. *J. Am. Chem. Soc.* **1969**, *91*, 5977.
(37) Gibson, D.; Johnson, B. F. G.; Lewis, J. *J. Chem. Soc. A* **1970**, 367. Simmons, M. G.; Merrill, K. C. C.; Wilson, L. J.; Bottomley, L. A.; Kadish, K. M. *J. Chem. Soc., Dalton Trans.* **1980**, 1827. Gagne, R. R.; Kreh, R. P. *J. Am. Chem. Soc.* **1979**, *101*, 6917. Kitagawa, S.; Munakata, M. *Inorg. Chem.* **1981**, *20*, 2261.
(38) Martell, A. E.; McCarthy, P. J. *Inorg. Chem.* **1967**, *6*, 781.
(39) Suguira, Y. *Inorg. Chem.* **1978**, *17*, 2176.
(40) Temussi, P. A.; Vitagliano, A. *J. Am. Chem. Soc.* **1975**, *97*, 1572.
(41) Kwik, W. L.; Ang, K. P. *J. Chem. Soc., Dalton Trans.* **1981**, 452.
(42) Treibs, A. *Justus Liebigs Ann. Chem.* **1929**, *1*, 476.
(43) Hill, H. A. O.; MacFarlane, A. J.; Williams, R. J. P. *J. Chem. Soc. A* **1969**, 1704. Hill, H. A. O.; Sadler, P. J.; Williams, R. P. J.; Barry, C. D. *Ann. N.Y. Acad. Sci.* **1973**, *206*, 247. Walker, F. A. *J. Magn. Reson.*, *15*, **1974**, 201. Barry, C. D.; Hill, H. A. O.; Mann, B. E.; Sadler, P. J.; Williams, R. J. P. *J. Am. Chem. Soc.* **1973**, *95*, 4545.
(44) Herbstein, F. H. *Perspectives in Structural Chemistry*; Dunitz, J. D., Ibers, J. A., Eds.; Wiley: New York, 1971; Vol. 4, pp 166–395.
(45) LaMar, G. N.; Fulton, G. P. *J. Am. Chem. Soc.* **1976**, *98*, 2119. LaMar, G. N.; Fulton, G. P. *J. Am. Chem. Soc.* **1976**, *98*, 2124. Abbott, E. H.; Rafson, P. A. *J. Am. Chem. Soc.* **1974**, *96*, 7378. Murray-Rust, P.; Wright, J. D. *J. Chem. Soc. A* **1968**, 247. Williams, R. M.; Wallwork, S. C. *Acta Crystallogr.* **1967**, *23*, 448. Kamenar, B.; Prout, C. K.; Wright, J. D. *J. Chem. Soc.* **1965**, 4851. Kamenar, B.; Prout, C. K.; Wright, J. D. *J. Chem. Soc.* **1966**, 661.

are limited. Scheidt[46] and co-workers have investigated a series of toluene-solvated first-row transition-metal complexes of 5,10,15,20-tetraphenylporphyrins. The interaction between the toluene and the metalloporphyrin involves both the central metal atom and a pyrrole ring. Schmitt's[47] perylene-bis[*cis*-1,2-bis(trifluoromethyl)ethene-1,2-dithiolato]nickel, perylene-Ni(tfd)$_2$, complex has the $\pi$ base situated symmetrically above the nickel thiolate, indicating direct metal atom-$\pi$-donor interaction.

Perhaps the most intriguing indication of an interaction between benzene and the copper-ketimine complexes is that the Cu-Cu distance in the binuclear complex decreases monotonically with increasing numbers of benzenes (Table IX). The Cu-Cu distance of 3.083 (1) Å for Cu$_2$(PAApr)$_2$ is the longest reported for any binuclear copper-ketonate complex[14,23-25,48] and is the only binuclear copper complex of this type completely lacking any significant axial interaction. Of the known five-coordinate copper-ketonate complexes with $\sigma$-donor axial ligands,[49] the range of Cu-Cu distances is 3.04-3.06 Å. The Cu-Cu distances for the benzene solvated structures summarized in Table IX are very similar to the five-coordinate copper binuclear ketonates with $\sigma$-axial ligands. One other geometric parameter that significantly changes throughout the solvated complexes tabulated above is the Cu-O(trans N) length. It varies 7$\sigma$ from the doubly solvated complex to the nonsolvated complex. As expected this length varies in the same direction as the Cu-Cu distance, although not so dramatically. Interestingly, it is the bridging oxygen atom that is centered in the projection of the Cu$_2$(PAAet)$_2$ complex onto the benzene plane (Figure 3), implying that this site is especially important in the $\pi$-molecular interaction.

**Acknowledgments** are made to the National Science Foundation (Grant CHE841-19100) for the purchase of a Syntex automated diffractometer and to the United States Air Force (Grant N00014-84-G-0211) for the purchase of a QE-300 multinuclear magnetic resonance spectrometer. The National Science Foundation (Grant CHE8300251) and the donors of the Petroleum Research Fund, administered by the American Chemical Society, are also acknowledged for the general support of this research. K.A.R. acknowledges support in the form of a Graduate Professional Opportunities Prgram Grant (GPOP).

**Registry No.** $H_2PAA$, 66734-21-2; Cu$_2$(PAAet)$_2$, 102869-03-4; Cu$_2$(PAAet)$_2$·$^1/_2C_6H_6$, 111769-79-0; Cu$_2$(PAApr)$_2$, 111742-38-2; Cu$_2$(PAAan)$_2$, 85319-02-4; Cu$_2$(PAApnan)$_2$, 85319-03-5; bis[2,2-dimethyl-7-(methylimino)-3,5-octanedionato]dicopper(II), 111742-45-1; bis[2,2-dimethyl-7-(butylimino)-3,5-octanedionato]dicopper(II), 111742-39-3; bis[2,2-dimethyl-7-(*p*-methylphenylimino)-3,5-octanedionato]dicopper(II), 111742-41-7; bis[2,2-dimethyl-7-(*p*-methoxyphenylimino)-3,5-octanedionato]dicopper(II), 111742-40-6; bis[2,2-dimethyl-7-(*p*-chlorophenylimino)-3,5-octanedionato]dicopper(II), 111742-42-8; bis[2,2-dimethyl-7-(*p*-bromophenylimino)-3,5-octanedionato]dicopper(II), 111742-44-0; bis[2,2-dimethyl-7-(*p*-(trifluoromethyl)phenylimino)-3,5-octanedionato]dicopper(II), 111742-43-9; methanamine, 74-89-5; ethanamine, 75-04-7; propanamine, 107-10-8; butanamine, 109-73-9; aniline, 62-53-3; *p*-methylphenylamine, 106-49-0; *p*-methoxyphenylamine, 104-94-9; *p*-chlorophenylamine, 106-47-8; *p*-bromophenylamine, 106-40-1; *p*-nitrophenylamine, 100-01-6; *p*-(trifluoromethyl)phenylamine, 455-14-1.

**Supplementary Material Available:** Tables of thermal parameters and hydrogen atom parameters for Cu$_2$(PAAet)$_2$·$^1/_2C_6H_6$ and Cu$_2$(PAApr)$_2$ (6 pages); listings of observed and calculated structure factors for both compounds (48 pages). Ordering information is given on any current masthead page.

(46) Scheidt, W. R.; Kastner, M. E.; Hatano, K. *Inorg. Chem.* **1978**, *17*, 706. Scheidt, W. R.; Reed, C. A. *Inorg. Chem.* **1978**, *17*, 710.
(47) Schmitt, R. D.; Wing, R. M.; Maki, A. H. *J. Am. Chem. Soc.* **1969**, *91*, 4394.
(48) Guthrie, J. W.; Lintvedt, R. L.; Glick, M. D. *Inorg. Chem.* **1980**, *19*, 2949.
(49) See ref 14, 23-25, 43.

Contribution from the Institut für Anorganische Chemie, Technische Hochschule Darmstadt, D-6100 Darmstadt, West Germany, and Laboratoire de Chimie des Métaux de Transition et de Catalyse associé au CNRS, Université Louis Pasteur, F-67008 Strasbourg, France

# Metal Complexes with Tetrapyrrole Ligands. 46.[1] Europium(III) Bis(octaethylporphyrinate), a Lanthanoid Porphyrin Sandwich with Porphyrin Rings in Different Oxidation States, and Dieuropium(III) Tris(octaethylporphyrinate)

Johann W. Buchler,*[2] André de Cian,[3] Jean Fischer,[3] Martina Kihn-Botulinski,[2] and Raymond Weiss*[3]

*Received June 4, 1987*

Reaction of tris(2,4-pentanedionato)europium(III) with octaethylporphyrin [$H_2$(OEP)] in refluxing 1,2,4-trichlorobenzene (TCB) produces a mixture of double-decker europium(III) bis(octaethylporphyrinate) [Eu(OEP)$_2$, **2**] and triple-decker dieuropium(III) tris(octaethylporphyrinate) [Eu$_2$(OEP)$_3$, **4**], which are separated by chromatography. **2** is characterized by UV/vis, near-IR, IR, $^1$H NMR, ESR, and mass spectra. Crystals of **2** (monoclinic, $P2_1/n$) are isomorphous with those of the known cerium(IV) sandwich Ce(OEP)$_2$ (**1**). The presence of Eu$^{III}$ follows from the temperature dependence of the magnetic moment. The well-defined composition Eu(OEP)$_2$ requires that one of the porphyrin rings is electron-deficient; i.e., the charge of the Eu$^{III}$ ion is compensated for by the normal porphyrinate dianion and a porphyrinate monoanion radical. The presence of a porphyrin radical is deduced from near-IR, IR, and NMR data, but the hole cannot be assigned to a specific ring on the time scales available. In refluxing TCB, **2** is transformed into **4** and $H_2$(OEP). Reduction of **2** with sodium anthracenide furnishes the anion [Eu(OEP)$_2$]$^-$.

Since the first observation of octacoordination in bis(acetato)zirconium(IV) and -hafnium(IV) porphyrins,[4] interest in porphyrin complexes with coordination number 8 has gradually increased. The bis($\beta$-diketonato) species M(P)(acac)$_2$[5] with M$^{IV}$ = Zr,[6] Hf,[6] Th,[7-9] and U[8] are well-defined compounds. The crystal

(1) Part 45: Buchler, J. W.; Herget, G. *Z. Naturforsch., B: Anorg. Chem., Org. Chem.* **1987**, 42B, 1003-1008.
(2) Technische Hochschule Darmstadt.
(3) Université Louis Pasteur.
(4) (a) Buchler, J. W.; Eikelmann, G.; Puppe, L.; Rohbock, K.; Schneehage, H. H.; Weck, D. *Justus Liebigs Ann. Chem.* **1971**, *745*, 135-151. (b) Hoard, J. L. In *Porphyrins and Metalloporphyrins*; Smith, K. M., Ed.; Elsevier: Amsterdam, 1975; pp 317-380. (c) Buchler, J. W. *Angew. Chem.* **1978**, *90*, 425-442; *Angew. Chem., Int. Ed. Engl.* **1978**, *17*, 403-423.
(5) Abbreviations used: M, metal; (P)$^{2-}$, (OEP)$^{2-}$, (Pc)$^{2-}$, (TPP)$^{2-}$, (TTP)$^{2-}$, and (TAP)$^{2-}$, dianions of a general porphyrin, 2,3,7,8,12,13,17,18-octaethylporphyrin, phthalocyanine, 5,10,15,20-tetraphenylporphyrin, 5,10,15,20-tetra-*p*-tolylporphyrin, and 5,10,15,20-tetra-*p*-anisylporphyrin, respectively; Ln, lanthanoid metal; H(acac), acetylacetone; HOAc, acetic acid; TCB, 1,2,4-trichlorobenzene; TLC, thin-layer chromatography; near-IR, near-infrared.
(6) Buchler, J. W.; Folz, M.; Habets, H.; van Kaam, J.; Rohbock, K. *Chem. Ber.* **1976**, *109*, 1477-1485.

0020-1669/88/1327-0339$01.50/0 © 1988 American Chemical Society